

## ***Supplementary Material***

The present Supplementary file presents data for: i) other analyzed cores (Table S1), ii) the Sea Surface Temperature (SST) residuals (Figure S1), iii) the appendix of planktonic Foraminifera species (Table S2, Figure S2), iv) the age model construction (Figure S3, Table S3 and Table S4), v) the sediment accumulation rates (Figure S5), vi) grain size analyses (Figure S4), as well as vii) the results of the ordinary least-squares regression (Table S5)

### **Cores location**

In the manuscript, Figure 1 shows the location of core SAT-048A, and the location of other mentioned cores as well. Names, coordinates, and depths below sea level for all cores are shown in Table S1.

**Table S1.** Location of the other analyzed cores, all of them recovered from the western South Atlantic.

Core	Lat	Long	Depth (mbsl)
GeoB2107-3	27° 10' S	46° 27' W	1048
GeoB2104-3	27.3° S	46.4° W	1500
SAT-048A	29° 11' S	47° 15' W	1542

### **SST<sub>100m</sub> estimates**

The SST estimates at 100 m below sea level (SST<sub>100m</sub>), performed on the present study, are shown in manuscript Figure 2e. Residual of this reconstruction is showed in Figure S1. The 95% of the residuals are located between 2.5 and -2.5°C, while the 90% are between 1.8 and -1.8°C.

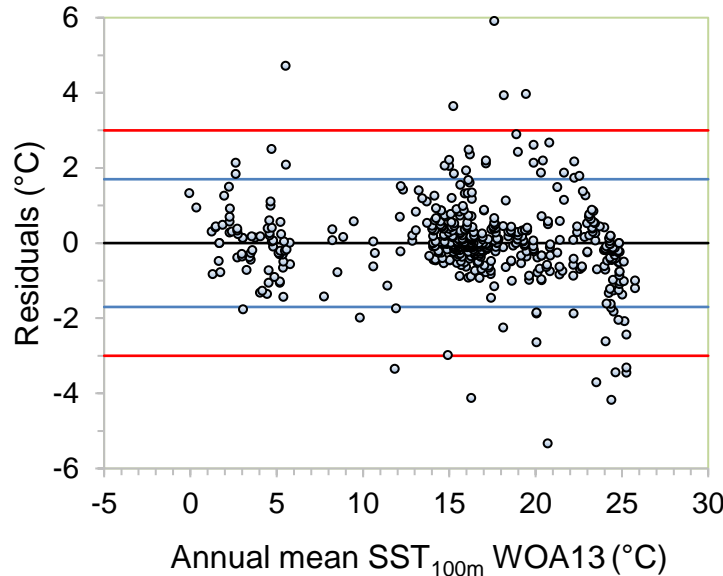


**Figure S1.** Residuals vs. Annual mean SST estimates at 100 m waters below sea level for core SAT048A. Red lines encompass 95% of the residuals (between 2.5 and -2.5°C) and blue lines encompass 90% (between 1.8 and -1.8°C).

### Planktonic Foraminifera abundances

From the 54 samples, a total of 21,962 specimens of planktonic Foraminifera were classified into 28 morphospecies. A total of 4878 specimens of benthic Foraminifera were counted. Table S2 lists the morphospecies, total relative abundance and total absolute abundance in descending order. The dominant species in the associations were *Globigerinoides ruber albus*, with a maximum relative abundance of 25.32%, followed by *Globigerinita glutinata* (15.56%) and *Globigerina bulloides* (15.56%). Other representative but less abundant species are *Neogloboquadrina incompta* (8.57%), *Globigerinoides ruber ruber* (8.22%) and *Globocanella inflata* (7.69%). Other species, with total relative abundances between 5 and 1% are (in decreasing order): *Trilobatus trilobus*, *Globoturborotalita tenellus*, *Neogloboquadrina dutertrei*, *Globorotalia scitula*, *Globoturborotalita rubescens*, *Globigerinella calida*, *Globorotalia truncatulinoides* (R), *Globorotalia crassaformis* and *Globorotalia truncatulinoides* (L). Finally, species with extremely low total absolute abundance (> 1%) are *Candeina nitida*, *Globigerina falconensis*, *Globigerinella siphonifera*, *Globigerinoides conglobatus*, *Globorotalia hirsuta*, *Globorotalia menardii*, *Globorotalia tumida*, *Neogloboquadrina pachyderma*, *Orbulina universa*, *Pulleniatina obliquiloculata*, *Trilobatus sacculifer*, *Turborotalita humilis* and *Turborotalita quinqueloba*.

**Table S2.** List of the species/morphospecies/subspecies identified and their total relative and absolute abundances.

Species/ Morphospecies/subspecies	Total relative abundance (%)	Total absolute abundance
<i>Globigerinoides ruber albus</i>	25.32	5573
<i>Globigerinita glutinata</i>	15.56	3391
<i>Globigerina bulloides</i>	15.56	3355
<i>Neogloboquadrina incompta</i>	8.57	1892
<i>Globigerinoides ruber ruber</i>	8.22	1828
<i>Globoconella inflata</i>	7.69	1701
<i>Trilobatus trilobus</i>	2.22	492
<i>Globoturborotalita tenellus</i>	2.22	480
<i>Neogloboquadrina dutertrei</i>	1.64	371
<i>Globorotalia scitula</i>	1.50	322
<i>Globoturborotalita rubescens</i>	1.46	314
<i>Globigerinella calida</i>	1.29	292
<i>Globorotalia truncatulinoides</i> (R)	1.28	295
<i>Globorotalia crassaformis</i>	1.28	289
<i>Globorotalia truncatulinoides</i> (L)	1.16	258
<i>Trilobatus sacculifer</i>	0.93	212
<i>Globigerina falconensis</i>	0.89	193
<i>Globorotalia hirsuta</i>	0.62	135
<i>Globigerinella siphonifera</i>	0.41	93
<i>Globorotalia menardii</i>	0.37	77
<i>Orbulina universa</i>	0.36	79
<i>Turborotalita quinqueloba</i>	0.32	67
<i>Globigerinoides conglobatus</i>	0.32	70
<i>Neogloboquadrina pachyderma</i>	0.24	54
<i>Pulleniatina obliquiloculata</i>	0.21	44
<i>Globorotalia tumida</i>	0.07	16
<i>Turborotalita humilis</i>	0.04	9
<i>Candeina nitida</i>	0.04	8

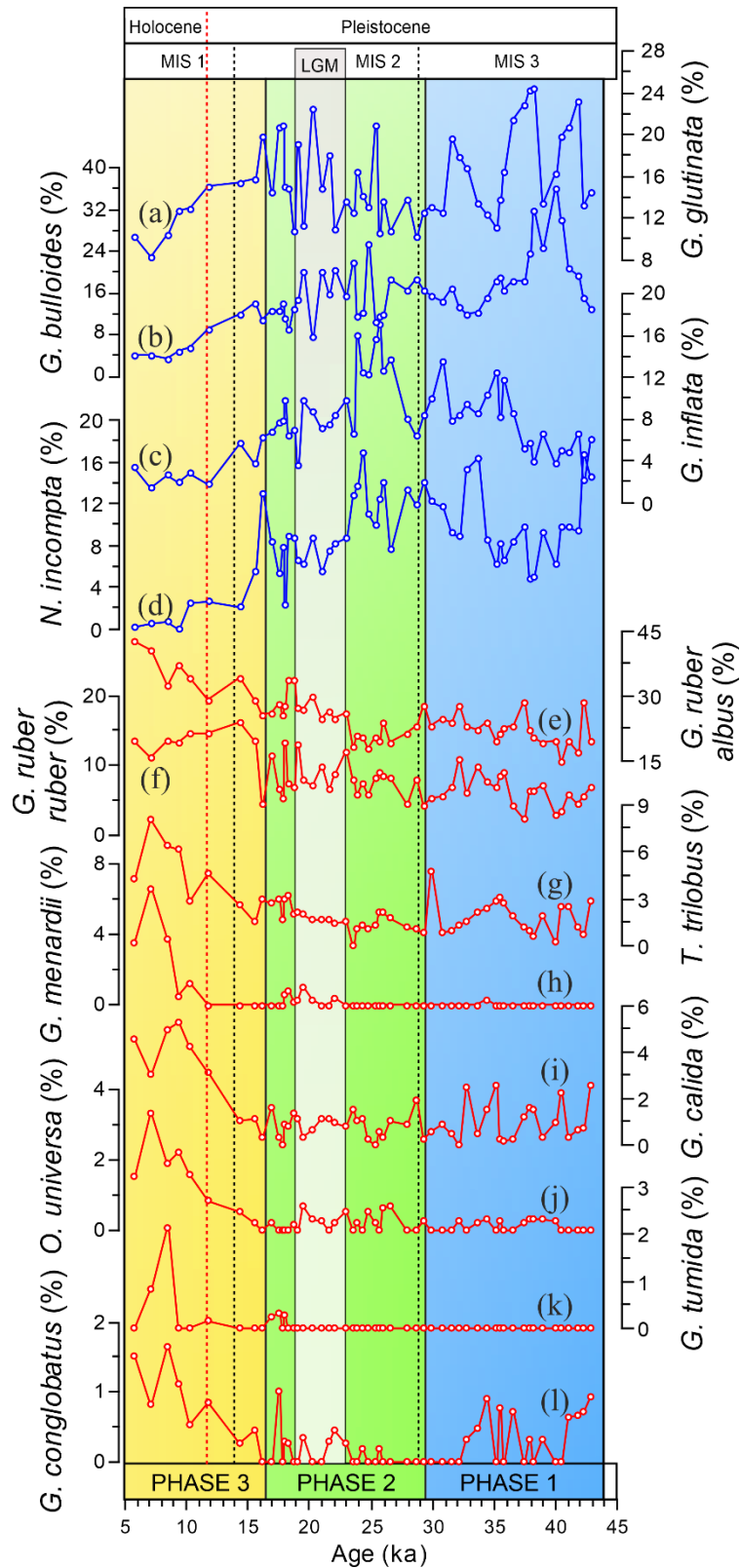


**Figure S2.** Relative abundances (%) of cool (A-D) and warm (E-L) water species (Kučera, 2007) along the core SAT-048A from the recovered period. (A) *G. glutinata*, (B) *G. bulloides*, (C) *G.*

*inflata*, (D) *N. Incompta*, (E) *G. ruber albus*, (F) *G. ruber ruber*, (G) *T. trilobus*, (H) *G. menardii*, (I) *G. calida*, (J) *O. universa*, (K) *G. tumida* and (L) *G. conglobatus*.

## Age Model

The performing results of the *rbacon* package for core SAT-048A are shown in Figure S3. It is possible to see the  $^{14}\text{C}$  correlation points, as wells as the identified Laschamp geomagnetic excursion (J. Savian, personal communication, June 5, 2020).

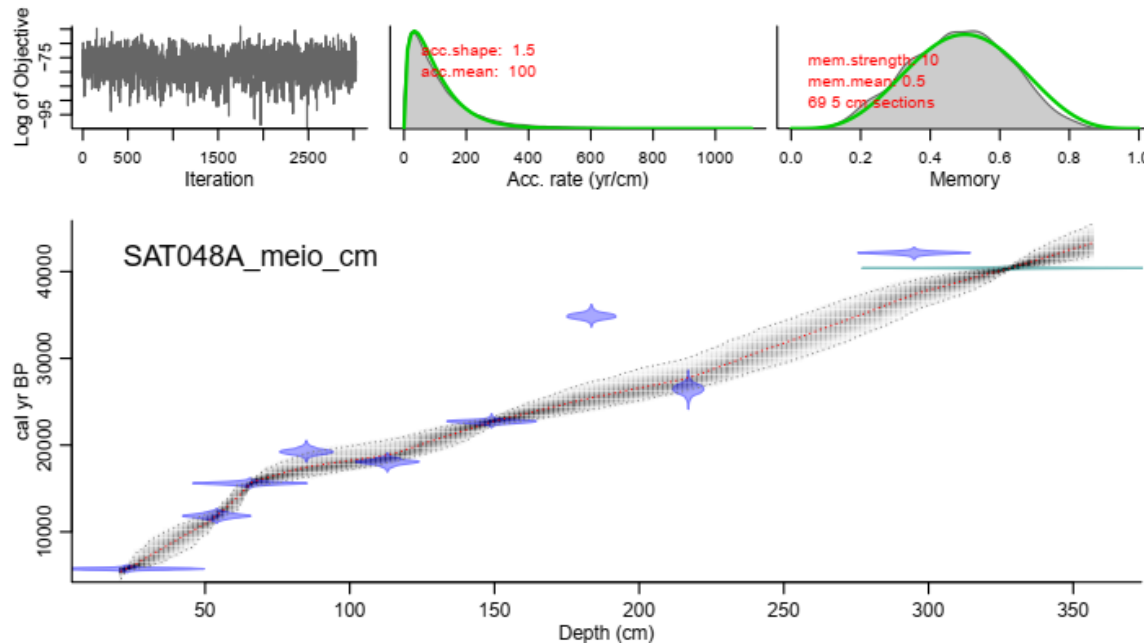


**Figure S3.** Age-depth plot for core SAT048A (bottom panel). The red stippled line indicates the mean age-depth model, 95% confidence ranges indicated by dark-grey stippled curves and calibrated dates in blue. Upper panels from left to right display (1) the Markov chain Monte Carlo (MCMC) iterations, the prior (green curves) and posterior (grey histograms) distributions for (2) the sedimentation rate and (3) memory.

The AMS  $^{14}\text{C}$  results of core SAT-048A (Frozza et al., 2020) are shown in Table S3. The Marine Reservoir Correction Database (Delta R = -85 +/- 40) is based on ages from Nadal de Masi (1999), Angulo et al. (2005), and Alves et al. (2015). *Rbacon* package (Blaauw & Christen, 2011; version 2.4.2), for open source R software (R Core Team, 2020), used the calibration curve Marine20 (Heaton et al., 2020). Table S4 shows data used for the age model (Figure S3) plus the Laschamp correlation point (J. Savian, personal communication, June 5, 2020).

**Table S3.** SAT-048A (Frozza et al., 2020) AMS  $^{14}\text{C}$  ages.

Sample depth (cm)	LAC-UFF sample code	Species	Age $^{14}\text{C}$ (ka BP)	Error (ka)
23	170059	<i>G. menardii</i>	5.226	0.028
23	170209	<i>G. ruber</i>	5.471	0.032
54	180167	<i>G. ruber</i>	10.594	0.117
65	190321	<i>G. ruber</i>	13.548	0.038
85	180168	<i>G. ruber</i>	16.599	0.212
113	180169	<i>G. ruber</i>	15.531	0.185
149	190704	<i>G. ruber</i>	19.536	0.104
183.5	190323	<i>G. ruber</i>	31.174	0.271
217	180170	<i>G. ruber</i>	22.997	0.451
295	190540	<i>G. ruber</i>	38.997	0.260

**Table S4.** SAT-048A data points for age model building on the “rbacon” package.

LabID	Age	Error	Depth_cm	cc	delta.R	delta.STD
LACUFF170059	5226	28	23	2	-85	40
LACUFF170209	5471	32	23	2	-85	40
LACUFF180167	10594	117	54	2	-85	40
LACUFF190321	13548	38	65.5	2	-85	40
LACUFF180168	16599	212	85	2	-85	40
LACUFF180169	15531	185	113	2	-85	40
LACUFF190704	19536	104	149	2	-85	40
LACUFF190323	31174	271	183.5	2	-85	40
LACUFF180170	22997	451	217	2	-85	40
LACUFF190540	38997	260	295	2	-85	40
Laschamp	41000	0	328	0	0	0

## Grain size analyses

Grain sizes were determined (for bulk samples and calcium carbonate-free samples) using a laser diffraction particle size analyzer Horiba Partica-LA-950. Calcium carbonate-free samples were analyzed after reaction with hydrochloric acid (HCl), 10%, at the Centro de Geologia Costeira e Oceânica (CECO), Universidade Federal do Rio Grande do Sul (UFRGS).

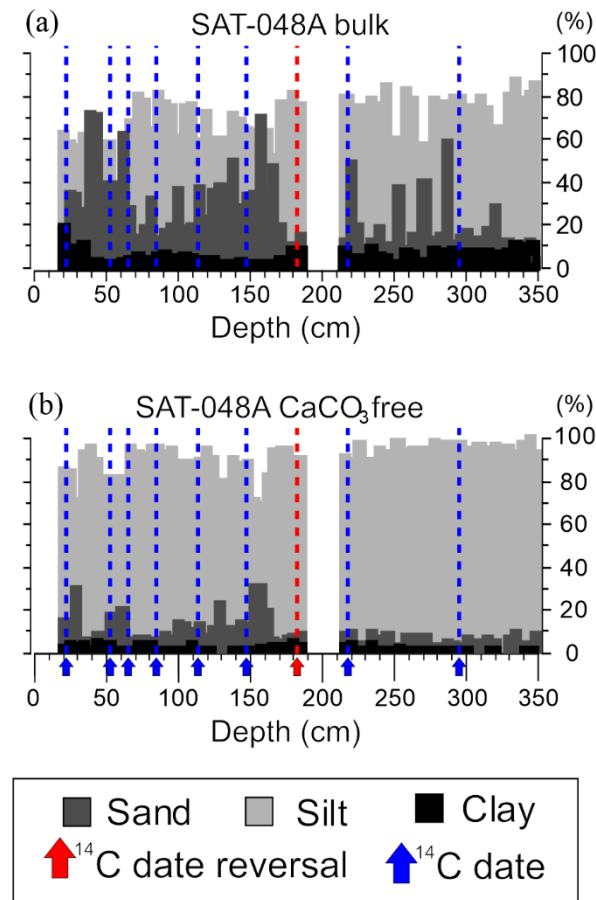


**Figure S4.** Results of grain sizes (bulk and CaCO<sub>3</sub> free) from core SAT-048A: sand (% , dark gray bars), silt (% , light gray bars) and clay (% , black bars) contents. Blue arrows and dotted lines represent the position of <sup>14</sup>C dates, while red arrow and dotted line indicate the most representative AMS <sup>14</sup>C reversal. The grain size record does not reveal abrupt shifts that could be related to sudden sedimentological processes.

## Sediment accumulation rates (SAR)

The age model suggests sedimentation rates varying between 2 and 20 cm/ky (Fig. S5).

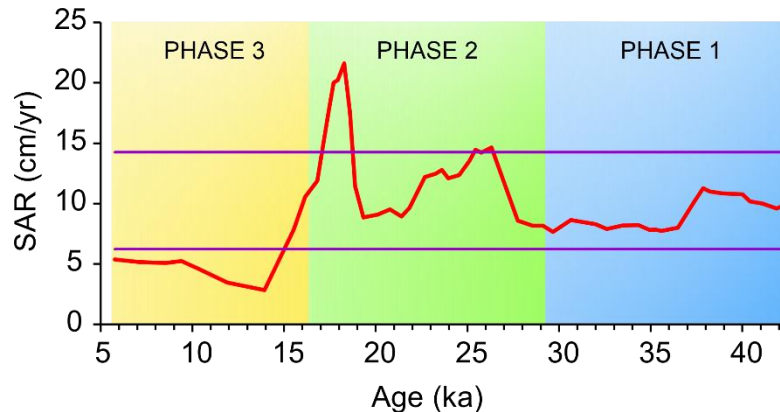


**Figure S5.** The sediment accumulation rates (cm/ky) through the timespan recorded by core SAT-048A shows variable values from 43 to 19 ka, a maxima peak at around 18 ka and decreases to a minimum at ka, remaining low until 5 ka. Red line is the calculated SAR and purple lines are the mean +/- standard deviation boundaries.

## Ordinary least-squares regression results

A full-factorial piecewise regression analysis was run to objectively determine the borders: (1) We calculated the regression line for a set of potential border scenarios (in total, 70 possible phase border combinations, Table S5). (2) For each regression line, we calculated the R<sup>2</sup> value (see table below). (3) The ideal phase border solution was determined as the one that would have the largest product of these three R<sup>2</sup> values.

**Table S5.** Individual R<sup>2</sup> values are shown for the 70 possible trial combinations. Best R<sup>2</sup> product is shown in bold.

Border 1/2	Border 2/3	R <sup>2</sup> _Phase1	R <sup>2</sup> _Phase2	R <sup>2</sup> _Phase3	Prod_R <sup>2</sup>
25.11	18.27	0.83	0.13	0.86	0.09
25.41	18.27	0.87	0.05	0.86	0.04
25.75	18.27	0.86	0.11	0.86	0.08
26.32	18.27	0.85	0.16	0.86	0.12
27.75	18.27	0.85	0.18	0.86	0.13
28.57	18.27	0.86	0.12	0.86	0.09
29.12	18.27	0.83	0.20	0.86	0.14
29.67	18.27	0.82	0.15	0.86	0.10
30.65	18.27	0.83	0.05	0.86	0.04
31.46	18.27	0.80	0.07	0.86	0.05
25.11	17.93	0.83	0.06	0.88	0.04
25.41	17.93	0.87	0.02	0.88	0.01

25.75	17.93	0.86	0.05	0.88	0.04
26.32	17.93	0.85	0.09	0.88	0.07
27.75	17.93	0.85	0.11	0.88	0.08
28.57	17.93	0.86	0.07	0.88	0.05
29.12	17.93	0.83	0.14	0.88	0.10
29.67	17.93	0.82	0.10	0.88	0.07
30.65	17.93	0.83	0.03	0.88	0.02
31.46	17.93	0.80	0.05	0.88	0.03
25.11	17.70	0.83	0.16	0.94	0.13
25.41	17.70	0.87	0.09	0.94	0.08
25.75	17.70	0.86	0.15	0.94	0.12
26.32	17.70	0.85	0.20	0.94	0.16
27.75	17.70	0.85	0.22	0.94	0.17
28.57	17.70	0.86	0.17	0.94	0.13
29.12	17.70	0.83	0.23	0.94	0.18
29.67	17.70	0.82	0.19	0.94	0.15
30.65	17.70	0.83	0.09	0.94	0.07
31.46	17.70	0.80	0.12	0.94	0.09
25.11	17.45	0.83	0.26	0.92	0.20
25.41	17.45	0.87	0.19	0.92	0.15
25.75	17.45	0.86	0.24	0.92	0.19
26.32	17.45	0.85	0.29	0.92	0.23
27.75	17.45	0.85	0.31	0.92	0.24
28.57	17.45	0.86	0.25	0.92	0.20
29.12	17.45	0.83	0.32	0.92	0.24
29.67	17.45	0.82	0.27	0.92	0.20
30.65	17.45	0.83	0.17	0.92	0.13
31.46	17.45	0.80	0.19	0.92	0.14
25.11	16.82	0.83	0.26	0.91	0.20
25.41	16.82	0.87	0.19	0.91	0.15
25.75	16.82	0.86	0.24	0.91	0.19
26.32	16.82	0.85	0.29	0.91	0.23
27.75	16.82	0.85	0.31	0.91	0.24
28.57	16.82	0.86	0.26	0.91	0.20
29.12	16.82	0.83	0.32	0.91	0.25
29.67	16.82	0.82	0.28	0.91	0.21
30.65	16.82	0.83	0.18	0.91	0.14
31.46	16.82	0.80	0.20	0.91	0.15
25.11	16.15	0.83	0.27	0.88	0.20
25.41	16.15	0.87	0.20	0.88	0.15
25.75	16.15	0.86	0.26	0.88	0.19
26.32	16.15	0.85	0.31	0.88	0.23
27.75	16.15	0.85	0.33	0.88	0.24
28.57	16.15	0.86	0.28	0.88	0.21
<b>29.12</b>	<b>16.15</b>	0.83	0.34	0.88	<b>0.25</b>

29.67	16.15	0.82	0.30	0.88	0.22
30.65	16.15	0.83	0.20	0.88	0.15
31.46	16.15	0.80	0.22	0.88	0.16
25.11	15.52	0.83	0.22	0.81	0.15
25.41	15.52	0.87	0.16	0.81	0.11
25.75	15.52	0.86	0.22	0.81	0.15
26.32	15.52	0.85	0.27	0.81	0.19
27.75	15.52	0.85	0.29	0.81	0.20
28.57	15.52	0.86	0.25	0.81	0.18
29.12	15.52	0.83	0.31	0.81	0.21
29.67	15.52	0.82	0.28	0.81	0.19
30.65	15.52	0.83	0.19	0.81	0.13
31.46	15.52	0.80	0.21	0.81	0.14

## References

- Alves, E., Macario, K., Souza, R., Pimenta, A., Douka, K., Oliveira, F., Chanca, I., & Ângulo, E. (2015). Radiocarbon reservoir corrections on the Brazilian coast from pre-bomb marine shells. *Quaternary Geochronology*, 29, 30–35. doi:10.1016/j.quageo.2015.05.006
- Angulo, R.J., de Souza, M.C., Reimer, P.J., & Sasaoka, S.K. (2005). Reservoir effect of the southern and southeastern Brazilian coast. *Radiocarbon*, 47, 67–73. doi:10.1017/S003382200052206
- Blaauw, M., & Christen, J.A. (2011). Flexible Paleoclimate Age-Depth Models using autoregressive gamma process. *Bayesian Analysis*, 6(3), 457–474. doi:10.1214/11-BA618
- Frozza, C.F., Pivel, M.A.G., Suárez-Ibarra, J.Y., Ritter, M.N., &, Coimbra, J.C., 2020. Bioerosion on late Quaternary planktonic Foraminifera related to paleoproductivity in the western South Atlantic. *Paleoceanography and Paleoclimatology*, 35, e2020PA003865. doi:10.1029/2020PA003865
- Heaton, T., Köhler, P., Butzin, M., Bard, E., Reimer, R., Austin, W., ... Skinner, L. (2020). Marine20—The Marine Radiocarbon Age Calibration Curve (0–55,000 cal BP). *Radiocarbon* 62 (4), 779–820. doi:10.1017/RDC.2020.68
- Lisiecki, L.E., & Stern, J.V. (2016). Regional and global benthic  $\delta^{18}\text{O}$  stacks for the last glacial cycle. *Paleoceanography*, 31 (10), 1368–1394. doi:10.1002/2016PA003002
- Nadal De Masi, M. A. (1999). Prehistoric hunter-gatherer mobility on the southern Brazilian coast: Santa Catarina Island. Ph.D. Thesis, Stanford University, Palo Alto, CA (unpublished).
- R Core Team. (2020). R: a language and environment for statistical computing. Vienna, Austria: R Foundation for Statistical Computing. <http://www.R-project.org/>

